

Comparison of field shifts in an atomic clock based on the effect of coherent population trapping in ^{87}Rb atoms under modulation of laser pump current at frequencies of 3.4 and 6.8 GHz

S.M. Ignatovich, M.N. Skvortsov, I.S. Mesenzova, L.N. Kvashnin,
V.I. Vishnyakov, D.V. Brazhnikov, S.N. Bagayev

Abstract. Experimental parameters of the resonance of coherent population trapping (CTP) on D1 line in ^{87}Rb and light shifts are compared under modulation of the laser pump current at frequencies of 3.4 and 6.8 GHz. Reproducibility of the parameters of a laser with a vertical cavity needed for long-term stability of an atomic clock is considered. The instabilities of atomic CPT-clock obtained for 1 s are 1.2×10^{-11} and 3×10^{-12} for frequencies of 3.4 GHz and 6.8 GHz, respectively.

Keywords: coherent population trapping, atomic clock, ^{87}Rb , modulation of laser pump current.

1. Introduction

Resonances of coherent population trapping (CTP) in alkali atoms are widely used for designing miniature atomic clocks [1–3]. CPT technology can substantially reduce size, required power, and cost of an atomic clock [4–8]. In many CPT-clocks, a vertical-cavity surface-emitting laser (VCSEL) is employed [9] with the pump current modulated by an oscillator at a frequency equal to half the hyperfine splitting frequency of the ground atomic state. In the single-mode regime, this modulation results in additional spectral components (side bands). Two side first-order bands are used for exciting a CPT-resonance according to the Λ -scheme. In ^{87}Rb , the hyperfine splitting of the ground state is 6.8 GHz for the D1 line, and, hence, the modulation frequency should be twice less, that is, 3.4 GHz. This modulation frequency is used in most of research groups. One more kind of modulation implies the modulation of laser pump current at a frequency equal to that of hyperfine splitting of the atomic ground state (6.8 GHz) [10, 11]. In this case, the CPT-resonance is excited according to the Λ -scheme by using a carrier and one of the first side emission bands. CPT-resonance may also be realised at other modulation frequencies of the pump current, which are multiples of the hyperfine splitting frequency of the atomic ground state. Nevertheless, at a higher multiplicity, the number of side bands increases, amplitudes of the spectral components participating in the two-photon Λ -scheme decrease, and

the rest components form a ‘pedestal’, which reduces the resonance contrast and increases the optical emission noise.

A short-term stability of an atomic clock is inversely proportional to the resonance width and is proportional to the signal-to-noise ratio, which is determined by the resonance contrast and noise of optical emission. The long-term stability is determined by various frequency shifts. The frequency shifts are studied as functions of operation parameters, such as the light intensity, power of the microwave signal that modulates the pump laser current, optical detuning from the optical transition frequency, absorbing cell temperature, buffer gas pressure in the cell, and external magnetic field.

In the present work, we present results of studying the parameters of CPT-resonance and light shifts for two cases of laser pump current modulation at frequencies of 3.4 and 6.8 GHz while observing the CPT-resonance on the D1 line in ^{87}Rb .

2. Experimental setup

A schematic of the experimental setup (Fig. 1) includes a VCSEL operating at a wavelength of 795 nm corresponding to the D1 line in ^{87}Rb . The laser is equipped with a precision power supply and temperature stabilisation system. The output radiation of the laser is linearly polarised and passes through a quarter-wave plate for obtaining circular polarisation. A gradient neutral optical filter is used for controlling the emission power. The filter is placed at a small angle to the laser output windows for preventing backward reflection to the laser. Having passed the plate, the radiation crosses an absorbing cell filled with rubidium vapours and a buffer gas. For observing absorption in alkali metal atoms, the cell is homogeneously heated to a temperature above 50 °C. Due to a specific design the cell windows have a lower temperature. Thus, metal condensates on the windows. This problem is solved by maintaining the cell temperature T_c by 5 °C higher than that of the fork T_f with metal rubidium inside.

Helmholtz coils are arranged on a cell case for producing a homogeneous magnetic field directed along wave-vectors of the wave. This field splits the energy levels of the ground state, which makes it possible to observe the CPT-resonance only related to the magnetic sublevels possessing quantum numbers $m_F = 0$, for which the linear Zeeman effect is absent. In addition, these levels undergo the shift quadratic in the magnetic field, which results in the corresponding shift of CPT-resonance (the frequency of the clock 0–0 transition)

$$\Delta\nu = K_0 B^2, \quad (1)$$

S.M. Ignatovich, M.N. Skvortsov, I.S. Mesenzova, L.N. Kvashnin,
V.I. Vishnyakov, D.V. Brazhnikov, S.N. Bagayev Institute of Laser
Physics, Siberian Branch, Russian Academy of Sciences, prosp. Akad.
Lavrent'eva 15B, 630090 Novosibirsk, Russia;
e-mail: mesenzova@yandex.ru

Received 13 January 2022
Kvantovaya Elektronika 52 (4) 386–390 (2022)
Translated by N.A. Raspopov

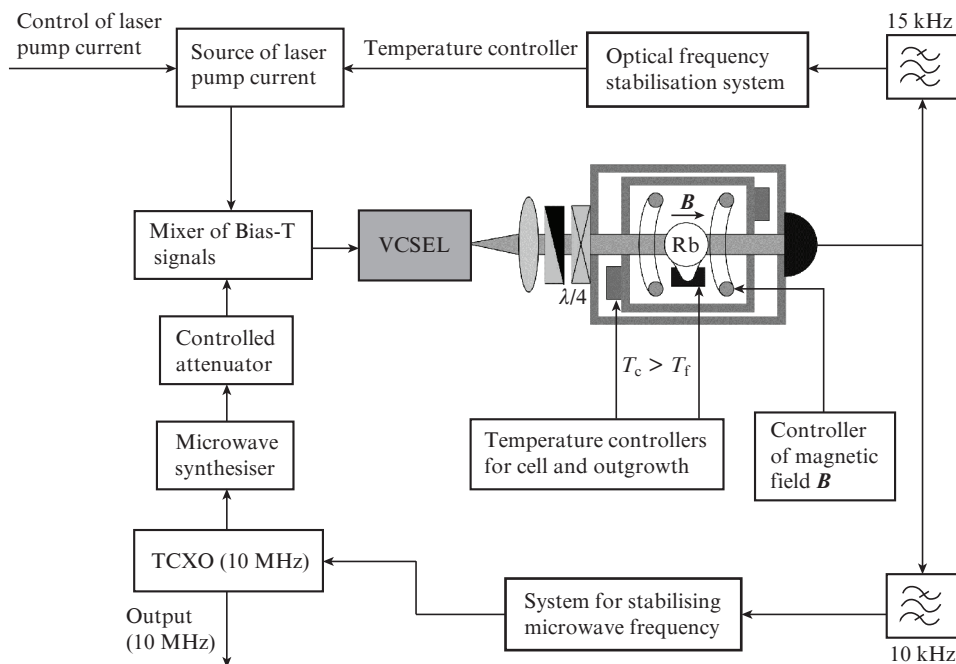


Figure 1. Schematic of the experimental setup for studying CPT-resonances on the D1-line in ^{87}Rb .

where B is the magnetic field induction (Gs). Issuing from the Breit–Rabi formula [12–14] one can show that for ^{87}Rb the factor of proportionality is $K_0 = 575.14 \text{ Hz Gs}^{-2}$. The value of the magnetic field in our case was 100–150 mGs.

In the case of two-photon (ν_1 and ν_2) interaction according to the Λ -scheme, the resonance optical frequencies in the laser emission spectrum were obtained by modulating the laser current at frequencies of 3.417 and 6.834 GHz. The modulation at the frequency of 3.4 GHz was realised by using an in-house developed microwave oscillator, which was incorporated into a miniature atomic clock. For modulation at 6.8 GHz, we used a high- and ultrahigh-frequency oscillator Roghde & Schwarz SMA-100B. Frequencies ν_1 and ν_2 are the ± 1 st order side frequencies of the formed frequency-modulated laser emission. In this case, the oscillation frequency is synthesised from a 10-MHz frequency of a thermo-compensated quartz oscillator (TCXO).

An automatic control system operating at a laser pump current modulation frequency of 15 kHz stabilises the laser optical emission frequency by the absorption D1-line of ^{87}Rb . The first harmonic of modulation frequency of the optical beam power, which passed through the rubidium cell, is synchronously detected for obtaining an error signal. The operation frequency value of the probe modulation (15 kHz) is chosen from considerations that both the laser and electronic components conventionally have no excess flicker noise at this frequency. The laser emission frequency can be controlled by varying the pump current or temperature. Variation of the pump current yields a much higher response speed as compared to a temperature change. However, the current variation strongly affects the laser output power, impedance, and modulation characteristics. In view of this fact, the error signal of the automatic control system is processed for tuning the laser temperature, whereas the probe modulation is realised through the laser current modulation. In addition, this approach compensates for the error of measuring a diode temperature by a sensor, which is related to different positions of the diode and sensor in space.

The frequency of the microwave oscillator is stabilised by a technique similar to the Pound–Drever–Hall method used for stabilising a laser frequency in the optical range [15]. In this method, the modulation frequency is much higher than the resonance width. In our case, the automatic control system employs the modulation frequency of ~ 9 kHz at the FWHM of observed CPT resonance 680 Hz. Such an approach has some advantages, namely, it provides the highest feedback response speed and makes it possible to choose a high operation frequency for improving the signal-to-noise ratio.

The absorbing cell is fabricated from quartz glass, which is alkali metal action-resistant and has a low gas permeability (for example, glass grade C51-1). The glass cell comprises pure isotope ^{87}Rb and a buffer inert gas (a mixture of argon and neon) at a pressure of ~ 100 Torr. Without buffer gas, the time of coherent interaction of rubidium atoms with a laser field is substantially shorter and equals the average time of atom flight through the beam, which substantially widens CPT resonances.

3. Experimental study of CPT-resonances on the D1 line in ^{87}Rb under modulation of the laser pump current at frequencies 3.4 and 6.8 GHz

The main sources of the long-term instability in miniature CPT-clocks are fluctuations of the following parameters:

- intensity of optical radiation;
- power of microwave modulation;
- collision shift due to buffer gas under variations of cell temperature;
- shift due to the variation of rubidium atom concentration caused by cell temperature changes; and
- shift determined by a magnetic field in the cell.

A change in the modulation frequency from 3.4 GHz to 6.8 GHz only affects the first two parameters. Sensitivity to

the rest fluctuations is independent of the modulation method [16].

The experimental setup makes it possible to observe CPT-resonances, measure their parameters, and determine (directly from the signal in the microwave stabilisation system) the slope of the frequency discriminator when the laser pump current is modulated at a frequency of 3.4 or 6.8 GHz. A characteristic view of the CPT-resonance in the case of the 6.8-GHz frequency is presented in Fig. 2, and the error signal in the microwave stabilisation system is shown in Fig. 3.

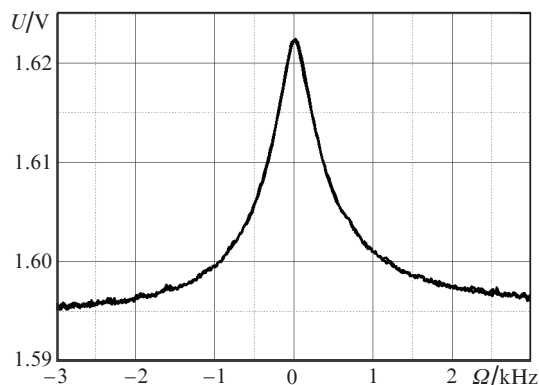


Figure 2. CPT-resonance.

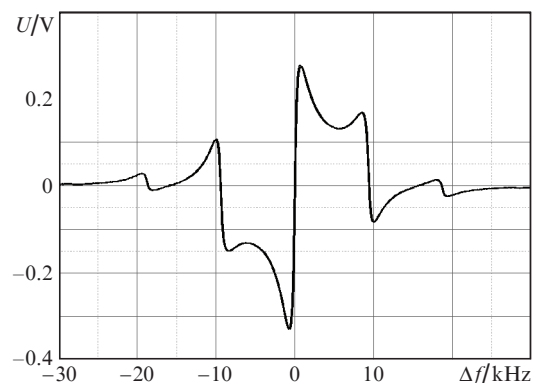


Figure 3. Error signal in the microwave frequency stabilisation system.

For studying the dependence of the field shifts of frequency on the microwave power, which modulates the laser pump current, the microwave frequency was stabilised by the frequency of the CPT-resonance, and the frequency of the atomic standard was measured relative to that of a hydrogen standard. In this case, the output frequencies (10 MHz) of the atomic standard based on ^{87}Rb and of the hydrogen time-frequency standard Ch1-1007 passed to a phase comparator-analyser VCH-323. The microwave power was measured stepwise; at each step the frequency of the atomic standard based on the CPT-resonance on the D1 line in ^{87}Rb was measured. Figure 4 presents measurement results for two VCSELs under the laser pump current modulated at a frequency of 3.4 GHz.

For one of the VCSELs [Fig. 4, curve (1)], the dependence has a minimum. This minimum was used in our earlier work [16] for enhancing the long-term stability of an atomic frequency standard. At this point, the first derivative of the fre-

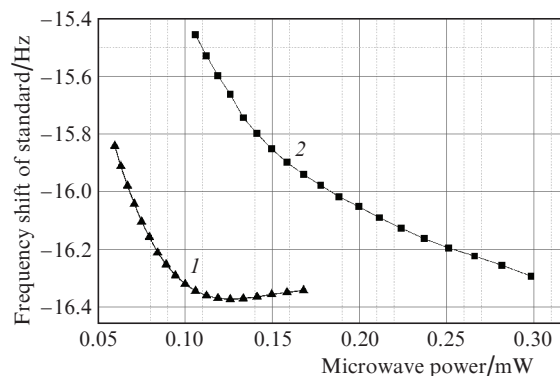


Figure 4. Frequency shift of the standard based on a CPT-resonance in ^{87}Rb for the line D1 as a function of the microwave power of two VCSELs (1, 2).

quency shift dependence on the microwave power is zero. With a VCSEL from the other series, such a point was not observed [Fig. 4, curve (2)]. In order to understand the difference between the lasers, we studied laser emission spectra on a scanning interferometer with the free spectral range of ~ 40 GHz.

As shown in Fig. 5, the spectra have side bands separated by the interval equal to the modulation frequency. In the laser with the observed minimum in the dependence of the frequency shift on the microwave power [Fig. 4, curve (1)], the spectrum looks much more symmetric (Fig. 5b).

For finding the optimal stabilisation parameters, the two main parameters of the CPT-resonance were studied: the slope of the frequency discriminator and the shift of the

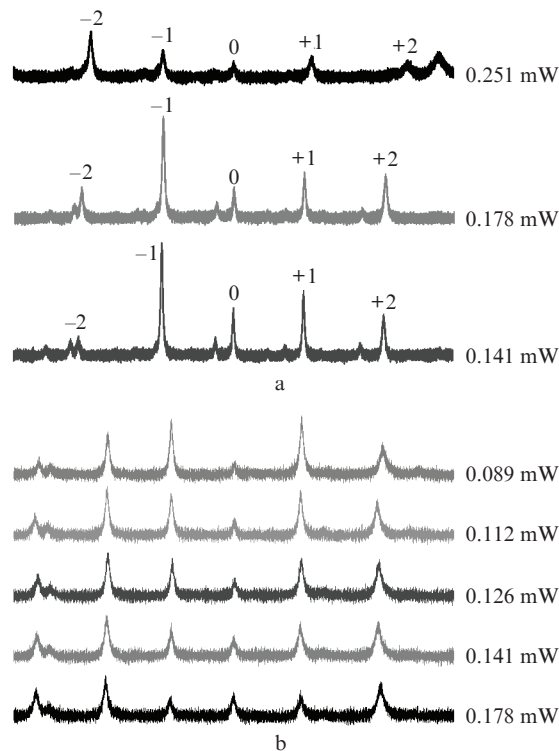


Figure 5. Laser emission spectra (a) without a zero-shift point and (b) with a zero-shift point at various values of microwave modulation.

atomic standard frequency calculated per 1% variation of the microwave power. Dependences of these parameters on the microwave power are shown in Fig. 6 for the case of the laser pump current modulation at a frequency of 3.4 GHz. The frequency shift of the atomic standard under microwave power variation by 1% of its operation value is calculated from the first derivative at any chosen operation point, multiplied by 0.01 of the power value at this point. The optimal (with respect to the microwave power) point for the long-term stability is the point where the power is $P_{\text{UHF}} = 0.16 \text{ mW}$, because at a small loss of the discriminator slope, the shift under variation of the microwave power is zero. This makes the standard low-sensitive to such a hardly controllable parameter as the amplitude of the microwave oscillator output signal.

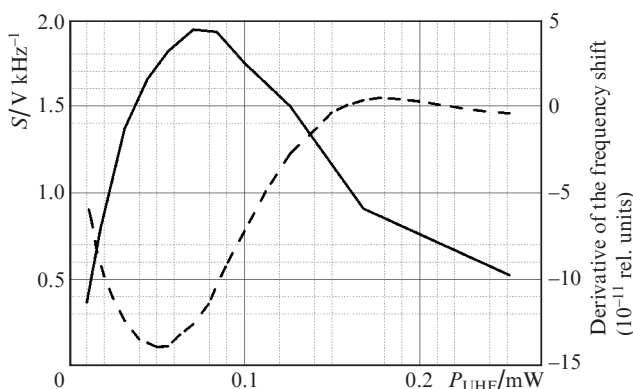


Figure 6. Slope S of the frequency discriminator (solid curve) and the frequency shift of the atomic standard as functions of the microwave power at the power variation by 1% (dashed curve) for the case of the laser pump current modulated at 3.4 GHz.

Similar investigations were performed under the modulation of the VCSEL pump current at a frequency of 6.8 GHz. First, emission spectra of lasers at the current modulation at 6.8 GHz were recorded by a scanning interferometer. Intensity distributions of the spectral components are shown in Fig. 7. Side bands are almost symmetrical.

Then, frequency shifts of the standard were studied at various optical field intensities with the modulation at a fre-

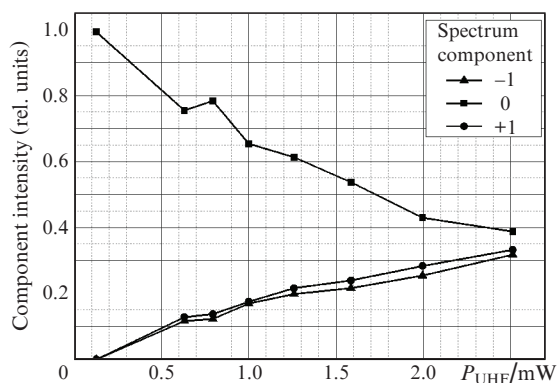


Figure 7. Intensities of side bands of laser emission with a pump current modulated at 6.8 GHz.

quency of 6.8 GHz. The measurements were taken for the three values of laser pump current: $J = 1.7, 1.5,$ and 1.3 mA . In addition, the Λ -scheme for observing the CPT-resonance in the case of VCSEL pump current modulation at a frequency of 6.8 GHz can be realised in the two variants: with the employment of a low-frequency side band and the central laser emission band or with a high-frequency side band and the central laser emission band. Measurement results for all the six cases are presented in Fig. 8.

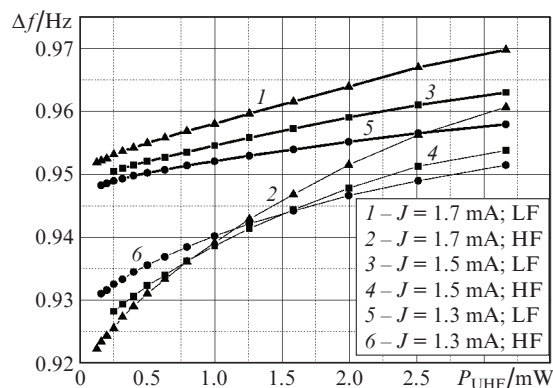


Figure 8. Field shifts of the frequency of the standard at a modulation of 6.8 GHz vs. microwave power at various laser pump currents. CPT-resonance was obtained from various components of the emission spectrum: LF-carrier + low-frequency side band, and HF-carrier + high-frequency side band.

One can see from Fig. 8 that the shifts are substantially less when the stabilisation is realised by the absorption line with the combination carrier + low-frequency side band (LF-regime), whereas in the HF-regime, the point of low sensitivity to variations of the laser pump current is observed. In view of the fact that the stability of a power supply is a well controllable parameter, the LF-regime is optimal for resonance observation.

For finding the optimal stabilisation regime from the viewpoint of obtaining the maximal signal-to-noise ratio while maintaining the minimal sensitivity to fluctuations of the optical field intensity, the parameters of CPT-resonances and the slope of frequency discriminators were studied in the case of laser pump current modulation at a frequency of 6.8 GHz. Figure 9 presents all measurement results for the slope of the frequency discriminator based on a CPT-resonance and for the shift of the frequency standard recalculated per 1% of the measured microwave power as functions of the microwave power.

In this case of modulation, a zero frequency shift was not observed, and the optimal laser operation regime was determined from the maximal slope of discriminator at the microwave power of 2.5 mW, which coincides with the microwave power corresponding to the minimal derivative of the frequency shift.

After the optimal stabilisation parameters have been chosen, an experiment on measuring Allan variance was performed for both the cases of modulation (Fig. 10). From Fig. 10, one can see that in the case of the 6.8-GHz frequency, a substantially lower short-term instability is observed (down to $\sim 3 \times 10^{-12}$ per 1 s). The long-term instability is explained

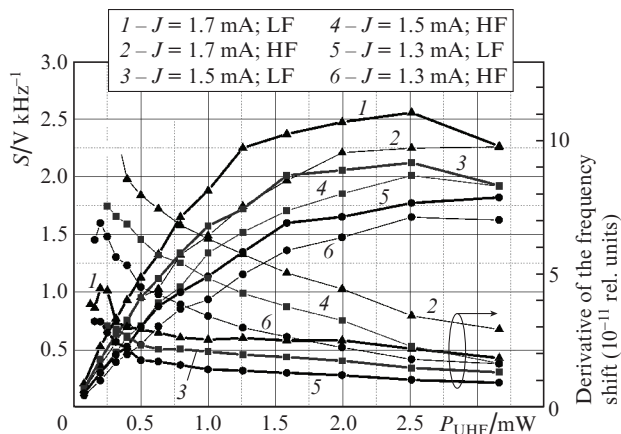


Figure 9. Slope S of the frequency discriminator and the frequency shift of the atomic frequency standard as functions of the microwave power under the power variation by 1% in the case of the laser pump current modulated at a frequency of 6.8 GHz.

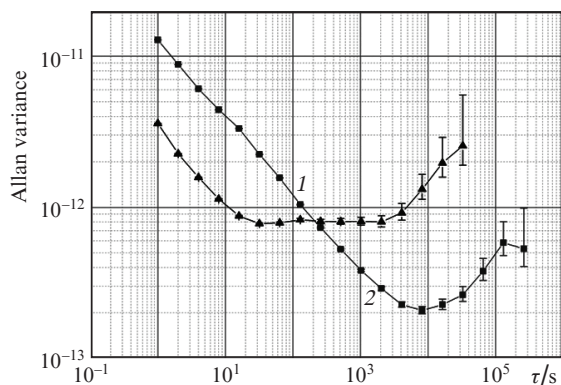


Figure 10. Allan variance for the cases of the laser pump current modulated at frequencies of (1) 6.8 and (2) 3.4 GHz.

by a relatively high temperature sensitivity of the microwave oscillator Roghde & Schwarz SMA-100B.

According to the formula from [17]

$$\delta\omega = \frac{1}{4} \frac{|\Omega_R|^2}{\Delta^2 + \gamma^2}, \quad (2)$$

the light shift $\delta\omega$ of resonance, obtained in the result of the interaction with off-resonant spectral components at a modulation frequency of 6.8 GHz should be less than the shift in the case of modulation at 3.4 GHz at similar component amplitudes. This reduces the sensitivity of the standard to a variation of the microwave power by 1% (Figs 6 and 9). In expression (2), Ω_R is the Rabi frequency; $\Delta = \omega_L - \omega_0$ is the detuning of laser frequency (ω_L from the resonance frequency (ω_0); and γ is the optical transition spectral width.

The total value of the light shift may slightly differ from calculated value because the light shift is affected by other factors not included in formula (2), for example, asymmetry of the resonance.

Authors of [11] thoroughly theoretically substantiated the reduction of shift characteristics and have shown that if a laser pump current is modulated at a frequency half the hyperfine splitting frequency, then the scheme becomes more sensitive to small variations in modulation parameters.

4. Conclusions

The comparison of the parameters of CPT-resonance on the D1 line of ^{87}Rb in the cases of laser pump current modulation at frequencies of 3.4 and 6.8 GHz has shown that the slope of the frequency discriminator based on the CPT-resonance at the optimal microwave power is the same for both frequencies. The study of field shifts of the frequency standard based on CPT-resonances demonstrates 2–4 times less field shifts in the case of laser pump current modulation at a frequency of 6.8 GHz. The short-term stability obtained (3×10^{-12} per 1 s) confirms promising applications of this approach for developing a miniature atomic clock.

Acknowledgements. The work was supported by the Russian Foundation for Basic Research (Grant No. 20-32-90029) and the Ministry of Science and Higher Education of Russian Federation (Presidential Grant No. SP-269.2021.3).

References

1. Knappe S. et al. *J. Opt. Soc. Am. B*, **18** (11), 1545 (2001).
2. Letokhov V.S., Chebotayev V.P. *Optical Science, Nonlinear Laser Spectroscopy* (Berlin: Springer-Verlag, 1977) Vol. 4.
3. Vanier J. *Appl. Phys.*, **81** (4), 421 (2005).
4. Kitching J. *Appl. Phys. Rev.*, **5**, 031302 (2018).
5. Knappe S., Schwindt P.D.D., Shah V., et al. *Opt. Express*, **13** (4), 1249 (2005).
6. Knappe S. et al. *Appl. Phys. Lett.*, **85** (9), 1460 (2004).
7. Zibrov S.A., Velichanskii V.L., Zibrov A.S., et al. *JETP Lett.*, **82**, 477 (2005) [*Pis'ma Zh. Eksp. Teor. Fiz.*, **82**, 534 (2005)].
8. Zibrov S.A., Novikova I., Phillips D.F., et al. *Phys. Rev. A*, **81**, 013833 (2010).
9. Michalzik R. *VCSELs* (Berlin–Heidelberg: Springer, 2013).
10. Goka S., Okura T., Moroyama M., Watanabe Y. *Proc. IEEE Int. Frequency Control Symp.* (Honolulu, Hawaii, USA, 2008).
11. Deng K., Guo T., Su J., Guo D., Liu X., Liu L., Chen X., Wang Z. *Phys. Lett. A*, **373**, 1130 (2009).
12. Breit G., Rabi I.I. *Phys. Rev.*, **38** (11), 2082 (1931).
13. Vanier J., Audoin C. *The Quantum Physics of Atomic Frequency Standards* (Bristol: Adam Hilger, 1989).
14. Miletic D. PhD Thesis (Université de Neuchâtel, 2013); <https://core.ac.uk/download/pdf/20662127.pdf>.
15. Drever R.W.P. et al. *Appl. Phys. B*, **31** (2), 97 (1983).
16. Skvortsov M.N. et al. *Quantum Electron.*, **50** (6), 576 (2020) [*Kvantovaya Elektron.*, **50** (6), 576 (2020)].
17. Deng J. *IEEE Trans. Ultrason. Ferroelec. Freq. Contr.*, **48** (6), 1657 (2001).